

# 3D reconstruction of vocal fold dynamics with laser high-speed videoendoscopy in children

Rita R. Patel PhD<sup>1</sup>  | Michael Döllinger PhD<sup>2</sup> | Marion Semmler PhD<sup>2</sup> 

<sup>1</sup>Department of Otolaryngology Head and Neck Surgery, Indiana University, Indianapolis, Indiana, USA

<sup>2</sup>Division of Phoniatrics and Pediatric Audiology at the Department of Otorhinolaryngology Head & Neck Surgery, University Hospital Erlangen, Friedrich-Alexander-Universität Erlangen-Nürnberg, Erlangen, Germany

## Correspondence

Rita R. Patel, Ph.D., CCC-SLP, Department of Otolaryngology Head and Neck Surgery, Indiana University School of Medicine, 1130 W. Michigan St., Fesler Hall, Suite 400, Indianapolis, IN 46202, USA.  
Email: [patelr@iu.edu](mailto:patelr@iu.edu)

## Funding information

Deutsche Forschungsgemeinschaft, Grant/Award Number: DO 1247/16-1; National Institute on Deafness and Other Communication Disorders, Grant/Award Number: R01DC017923

## Abstract

**Objective:** The objective of this study is to evaluate three-dimensional vertical motion of the superior surface of the vocal folds in vivo in (a) typically developing children as a function of vocal frequency variations and (b) a child with vocal nodules.

**Methods:** A custom developed laser endoscope coupled with high-speed videoendoscopy was used to obtain 3D parameters from 2 healthy children, one child with vocal nodules, and 23 vocally healthy adults (females = 11, males = 12). Parameters of amplitude (mm), maximum opening/closing velocity (mm/s), and mean opening/closing velocity (mm/s) were computed for the lateral and vertical vibratory motion along the anterior, middle, and posterior sections of the vocal folds were computed.

**Results:** We provide for the first time, absolute measurements of vertical amplitude and maximum/ mean velocity during the opening and closing phases, in vivo in children. Overall, the vertical motion was larger in vocally normal children compared with the lateral motion, especially along the visible posterior section of the vocal folds and during low pitch phonation. The opening phase dynamics were consistently large along the posterior section in the child with vocal nodules.

**Conclusions:** The study findings establish the feasibility of capturing 3D motion in a clinical setting and provide proof of concept for the application of the proposed 3D laser in the pediatric population. Future large sample size studies are needed to establish the diagnostic potential of examining the closing phase vertical motion to evaluate vibratory development in children with normal voice and investigating the opening phase vertical motion in children with nodules.

**Level of Evidence:** N/A.

## KEYWORDS

high-speed videoendoscopy, laser endoscopy, pediatrics, three-dimensional imaging

## 1 | INTRODUCTION

Videostroboscopy, the current gold-standard for laryngeal endoscopic examination clinically,<sup>1,2</sup> is limited with regard to examination of highly unstable and severely disordered voices.<sup>3,4</sup> Over the past two

decades, there has been widespread utilization of high-speed videoendoscopy to gain robust insights into aperiodic, short duration vocal fold vibratory motion; both in healthy adults<sup>5-11</sup> and those with voice disorders.<sup>3,12-15</sup> More recently, there is emerging evidence of the usefulness of high-speed videoendoscopy in gaining comprehensive

This is an open access article under the terms of the [Creative Commons Attribution-NonCommercial-NoDerivs](https://creativecommons.org/licenses/by-nc-nd/4.0/) License, which permits use and distribution in any medium, provided the original work is properly cited, the use is non-commercial and no modifications or adaptations are made.

© 2024 The Author(s). *Laryngoscope Investigative Otolaryngology* published by Wiley Periodicals LLC on behalf of The Triological Society.

insights into the dynamics of vocal fold motion in children with<sup>16–18</sup> and without<sup>17,19–23</sup> voice disorders. Laryngeal endoscopic examination with either videostroboscopy or high-speed videoendoscopy only provides information of vocal fold motion in 2-dimension (2D).

Recent examination with custom developed grid laser projection unit coupled with high-speed videoendoscopy has demonstrated the feasibility<sup>24–26</sup> and utility<sup>27,28</sup> of quantifying not only the lateral<sup>29–31</sup> motion but also the vertical<sup>24,27,28,32</sup> motion of the superior surface of the vocal folds in adults. Although data from adults are valuable it cannot be directly applied to evaluate pediatric voices due to substantial differences in laryngeal anatomy and vocal fold histoarchitecture between children and adults. Children typically have shorter vocal folds and underdeveloped deep layers of the vocal folds.<sup>33–39</sup> Children have higher prevalence of posterior phonatory gap,<sup>40</sup> a larger amplitude-to-length ratio,<sup>23</sup> a longer longitudinal phase delay between the anterior and posterior parts of the vocal folds during the opening phase,<sup>19</sup> and greater cycle-to-cycle variability<sup>21</sup> compared with typical adults. Given these substantial changes in vocal anatomy and physiology, the purpose of this study is to quantify the vertical motion of the superior

surface of the vocal folds in typically developing children and a child with vocal fold nodules. To the best of our knowledge, there are no studies quantifying the superior surface vocal fold vertical motion in children.

Studies utilizing laser projection unit in children have thus far utilized two-point laser<sup>41</sup> or multiple vertical stripes<sup>42</sup> to quantify lateral motion of the vocal folds and lesion size<sup>43</sup>/landmarks of interest. The laser projection unit with the multiple stripes though small had low contrast, which limited the visibility of the stripe patterns at faster frame rates associated with high-speed videoendoscopy. The proposed laser in the study has a grid of  $18 \times 18$  dots and is visible at high frame rates of up to 4000 frames per second. The current study extends our prior work on quantitative evaluation of vocal fold vibratory motion in children, by evaluation the 3D vibratory motion of the superior surface of the vocal folds. The goal of the study is to evaluate how the 3D laser high-speed videoendoscopy parameters vary along the anterior, middle, and posterior margins of the vocal folds (a) as a function of low, middle, and high pitch in vocally healthy children compared with adults and (b) in a child with vocal nodules compared with vocally healthy children.

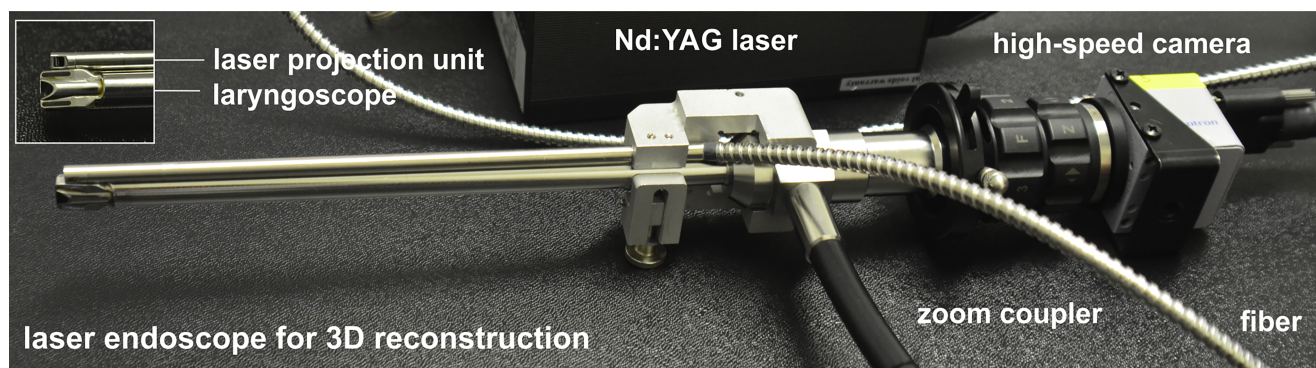


**FIGURE 1** Custom developed laser set-up with high-speed videoendoscopy for in-vivo measurement of three-dimensional vocal fold motion in children.

**TABLE 1** Mean and standard deviation of vocal pitch (Hz) and vocal sound pressure level (dB SPL) across high pitch (80% of the pitch range), typical pitch (20% of the pitch range), and low pitch (10% of the pitch range) for vocally normal children ( $n = 2$ , 1 boy, 1 girl), females ( $n = 11$ ), and males ( $n = 12$ ). One child with vocal fold nodules was also included.

	Vocal pitch (Hz)			Vocal sound pressure level (dB (C) SPL@30 cm)		
	HPNL	NPNL	LPNL	HPNL	NPNL	LPNL
Female adults	431.78 $\pm$ 82.68 ( $n = 10$ )	241.76 $\pm$ 25.42 ( $n = 11$ )	217.90 $\pm$ 14.09 ( $n = 10$ )	75 $\pm$ 6.46 ( $n = 10$ )	70.18 $\pm$ 4.04 ( $n = 11$ )	68.5 $\pm$ 3.73 ( $n = 10$ )
Male adults	239.41 $\pm$ 73.80 ( $n = 12$ )	124.25 $\pm$ 18.76 ( $n = 12$ )	113.33 $\pm$ 18.20 ( $n = 10$ )	77.75 $\pm$ 4.46 ( $n = 12$ )	73.08 $\pm$ 2.78 ( $n = 12$ )	71.1 $\pm$ 4.27 ( $n = 10$ )
Children	431.94 $\pm$ 71.53	270.31 $\pm$ 27	240.82 $\pm$ 24.04	71 $\pm$ 5.77	71 $\pm$ 3.46	65 $\pm$ 1.15
Child with nodule	–	314	–	–	72	–

Note: dB (C) SPL@30 cm = calibrated sound pressure level in decibels using C-weighted scale with mouth-to-microphone distance at 30 cm from the mouth.

Abbreviations: HPNL, high pitch normal loudness; LPNL, low pitch normal loudness; NPNL, normal pitch normal loudness.

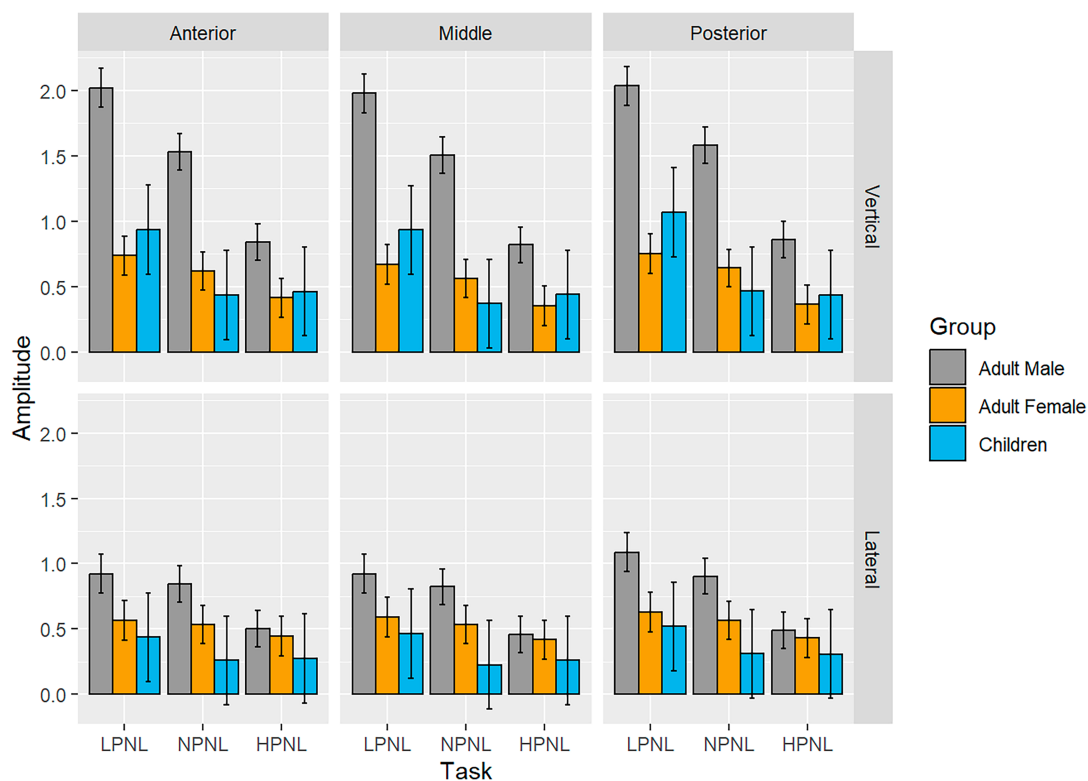


**FIGURE 2** Estimated mean and standard error of amplitude (mm) in the lateral and vertical directions along the anterior, middle, and posterior sections of the vocal folds for low pitch normal loudness (LPNL), normal pitch normal loudness (NPNL), and high pitch normal loudness (HPNL) in males ( $n = 12$ ), females ( $n = 11$ ), and children ( $n = 2$ ).

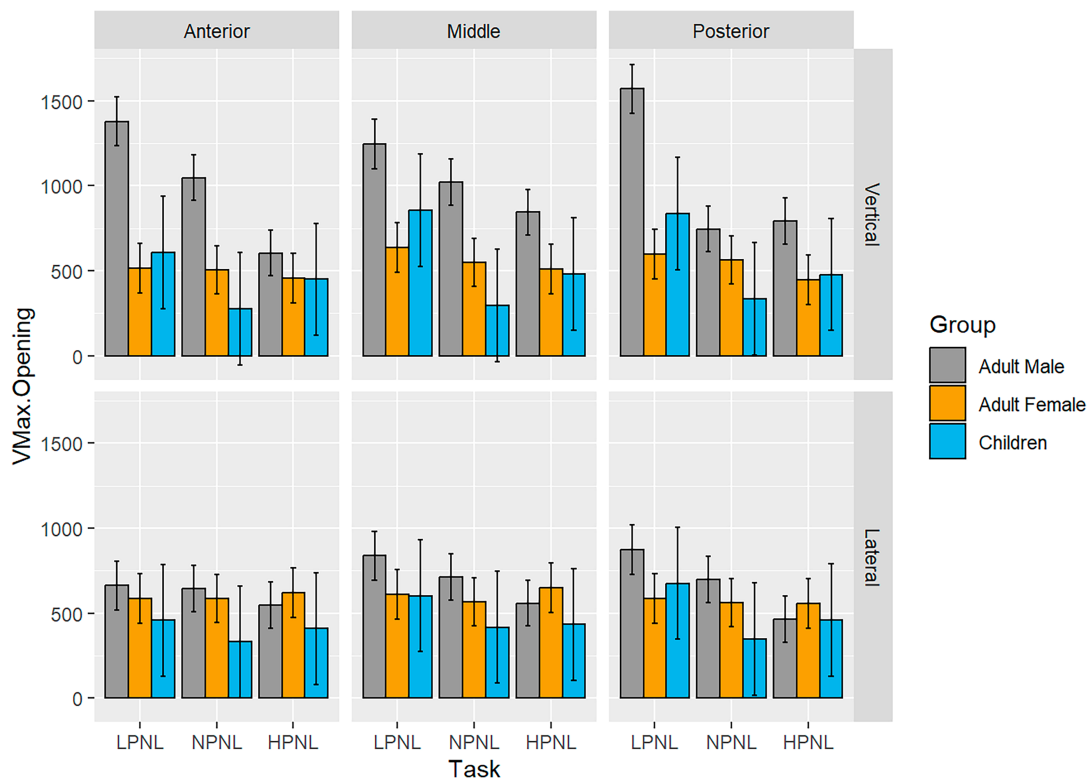


**FIGURE 3** Estimated mean and standard error of maximum velocity for the opening phase (mm/s) in the lateral and vertical directions along the anterior, middle, and posterior sections of the vocal folds for low pitch normal loudness (LPNL), normal pitch normal loudness (NPNL), and high pitch normal loudness (HPNL) in males ( $n = 12$ ), females ( $n = 11$ ), and children ( $n = 2$ ).

## 2 | METHODS

### 2.1 | Laser endoscope

A custom laser projection unit (LPU) attachment (Bayerisches Laserzentrum GmbH, Erlangen, Germany) to a rigid 10 mm 70° endoscope was developed in collaboration with the University of Erlangen, Germany (Figure 1). The LPU is 5 mm wide and provides an output power of 150 mW and a wavelength of 532 nm.<sup>24,27,28</sup> The laser dots (18 × 18 grid) are <0.25 mW with an average size of 0.25 mm<sup>2</sup> at 60 mm distance between the tip of the endoscope and the vocal folds.<sup>28</sup> The LPU calibration using ex-vivo experiments revealed a mean bias of 0.11 ± 0.04 mm in the vertical direction and a precision of 0.15 ± 0.04 mm.<sup>24</sup> Further information about the laser system is presented in Semmler et al 2016,<sup>24</sup> 2017,<sup>28</sup> and 2018.<sup>27</sup>

### 2.2 | Data collection

Both adult and child participants were recruited at the Vocal Physiology and Imaging at Indiana University. Prior to conducting the study, IRB approved consent and assent forms were obtained. Three child

participants between the ages of 7 and 9 years (males = 2, females = 1) were included in the study. One of the male child participants had vocal fold nodules. The remainder of the child participants had a normal voice and did not display any vocal fold abnormalities. To compare 3D data from typically developing children to vocally normal adults and determine where the children lie in relation to the developmental endpoint, we utilized our previously published data from 23 vocally healthy adults, 12 males (24.80 ± 4.11 years) and 11 females (23.83 ± 2.76 years).<sup>32</sup>

Prior to laser endoscopy, participants pitch range was recorded using a glide from the lowest to the highest pitch, with a stable loudness, using an omnidirectional microphone (Shur Beta 53) placed at a 45° angle at a distance of 4 cm from the corner of the mouth.<sup>2</sup> The pitch range was used to determine each participant's habitual (20% of the entire pitch range), low (10% of the entire pitch range), and high pitch (80% of the entire pitch range). All participants were subsequently trained to produce sustained /i:/ at 10%, 20%, and 30% of the pitch range; except the child with vocal nodules was only able to produce phonation at habitual/middle pitch level. The Photron FASTCAM MC2 (PENTAXMedical, Montvale New Jersey) high-speed camera was used to capture vocal fold vibrations at 4000 frames per second with the spatial resolution of 512 × 256 pixels.

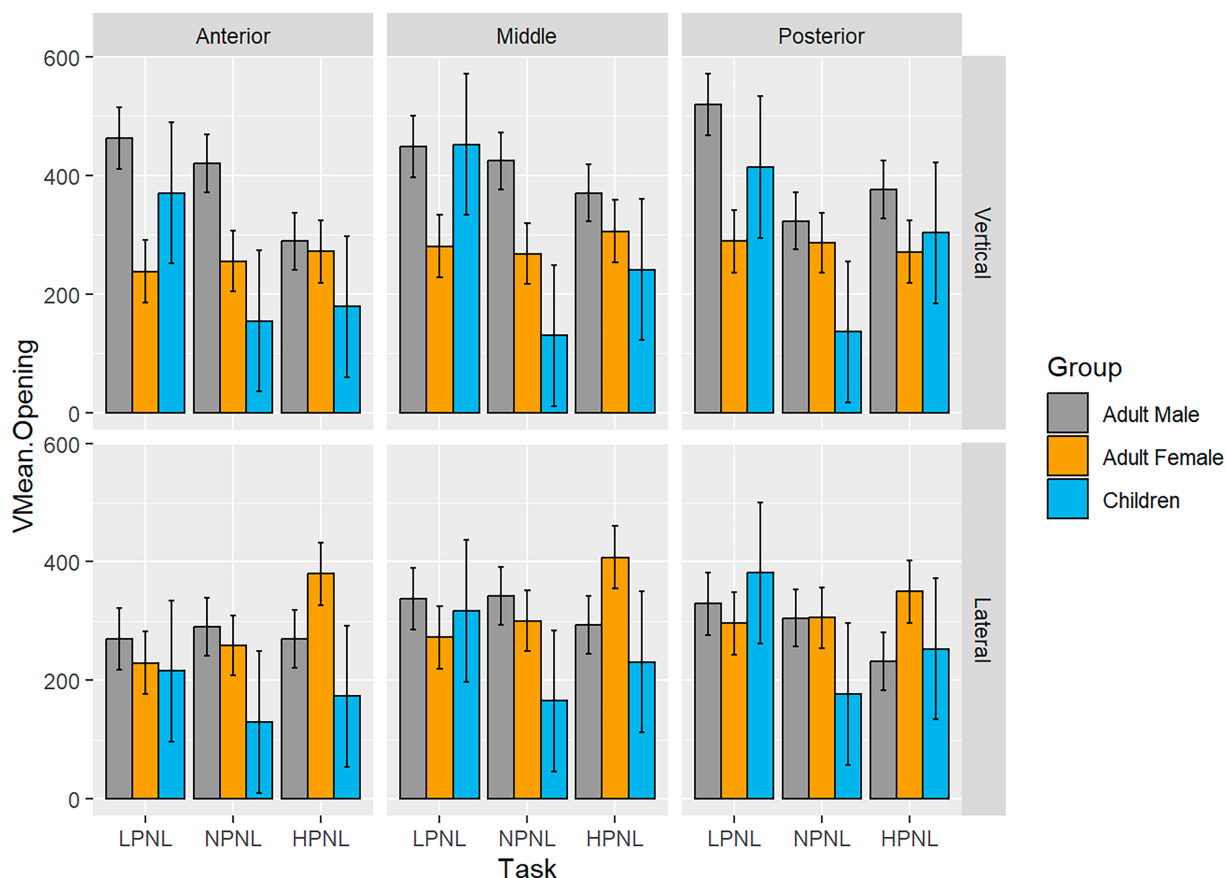


**FIGURE 4** Estimated mean and standard error of mean velocity for the opening phase (mm/s) in the lateral and vertical directions along the anterior, middle, and posterior sections of the vocal folds for low pitch normal loudness (LPNL), normal pitch normal loudness (NPNL), and high pitch normal loudness (HPNL) in males ( $n = 12$ ), females ( $n = 11$ ), and children ( $n = 2$ ).



## 2.3 | Data analyses

A custom-developed laser endoscope coupled with high-speed videoendoscopy utilizing stereo triangulation was used to obtain a three-dimensional motion of the vocal folds during phonation. Two-dimensional segmentation of the high-speed video recordings from 500 frames was first obtained using the Glottis Analysis Tools (v. 2018, Erlangen, Germany).<sup>44,45</sup> A semi-automated custom developed software called VideoClick (v.2. Erlangen, Germany)<sup>28</sup> was subsequently used for three-dimensional reconstruction. The tracking of points was verified by a trained observer. In instances where the automated tracking was not accurate, the points were manually tracked and/or corrected for concerned frames.

## 2.4 | Parameters

The reconstructed 3D data points were interpolated using bicubic splines from the superior surface of the vocal folds.<sup>24,27,28</sup> The 3D parameters of amplitude (mm), maximum velocity (mm/s), and mean velocity (mm/s) were computed for the lateral and vertical vibratory

motion along the anterior, middle, and posterior sections of the vocal folds. The vertical amplitude refers to the maximum displacement vertically. The maximum change between two successive frames divided by the frame duration during the opening phase determines the maximum vertical velocity during opening and during the closing phase is the maximum vertical velocity during closing. The maximum lateral excursion from the closed vocal folds was computed as the lateral maximum amplitude. The lateral velocity was recalculated based on the lateral displacement observed throughout the recording duration. A comprehensive description of the parameter calculations is found in Semmler et al.<sup>27</sup>

## 2.5 | Statistical analyses

Linear mixed model was conducted to evaluate the differences in (a) vocal frequency task, (b) axis level, and (c) position level (anterior vs. middle vs. posterior) in (I) typically developing children vs. adults and (II) typically developing children vs. child with vocal nodules on the 3D HSV outcome variables, with participant as random effect. Pairwise comparisons were adjusted using the Tukey test. *p*-values

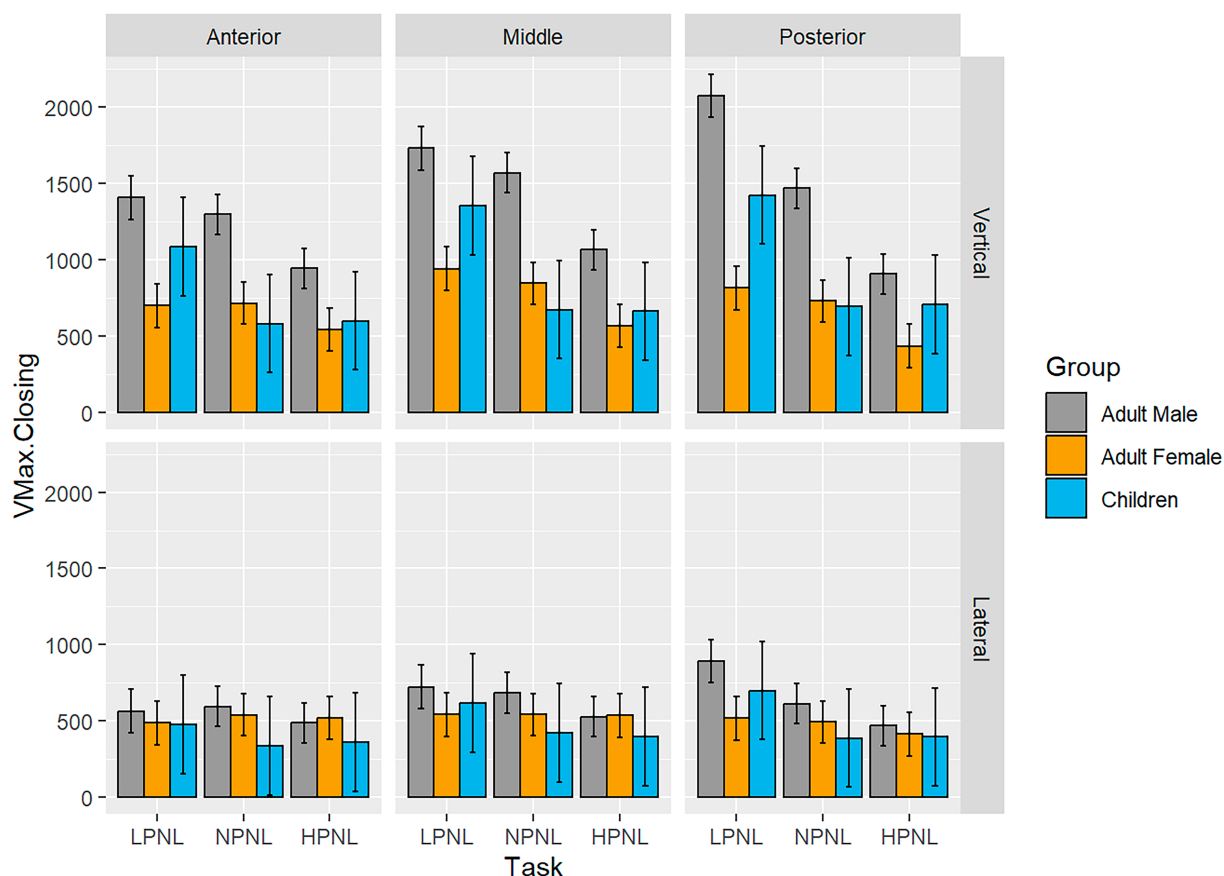


**FIGURE 5** Estimated mean and standard error of maximum velocity for the closing phase (mm/s) in the lateral and vertical directions along the anterior, middle, and posterior sections of the vocal folds for low pitch normal loudness (LPNL), normal pitch normal loudness (NPNL), and high pitch normal loudness (HPNL) in males ( $n = 12$ ), females ( $n = 11$ ), and children ( $n = 2$ ).

were two-tailed and considered significant at values  $<0.05$ . All analyses were performed using R, version 4.2.2.

### 3 | RESULTS

The mean and standard deviation of vocal frequency (Hz) and vocal sound pressure level (dB SPL) across the three tasks of high pitch, normal pitch, and low pitch are depicted in Table 1.

#### 3.1 | Children compared with adults

##### 3.1.1 | Amplitude (mm)

The main effects of group, axis, and task were significantly associated with ( $p < .001$ ) amplitude (mm), where the amplitude was consistently larger for adult males, larger in the vertical axis compared with the lateral axis, and larger for low pitch (Figure 2). Significant difference was not obtained for the anterior, middle, and posterior positions ( $p = .943$ ), suggesting that the amplitude is similar across the three positions as a function of pitch.

The difference in the amplitude across the groups depends on the axis as the interactions  $axis \times group$  ( $p = .001$ ) and  $task \times axis$  ( $p = .008$ ) were significant. The amplitude was significantly larger in the vertical direction for only males ( $p < .001$ ) and not significant for females ( $p = .976$ ) and children ( $p = .294$ ) when compared with lateral motion. The amplitude was significantly larger for males when compared with females during the low pitch ( $p < .001$ ), typical pitch ( $p = .002$ ), but not for high pitch ( $p = .605$ ).

The amplitude was significantly larger in males when compared with children for typical pitch ( $p = .032$ ) but not for low pitch ( $p = .075$ ) and high pitch ( $p = .944$ ).

The amplitude was not significantly larger in females when compared with children during the low pitch production ( $p = 1$ ), normal pitch ( $p = .988$ ), or high pitch ( $p = 1$ ).

##### 3.1.2 | Maximum opening velocity (mm/s)

There were significant main effects of axis, task, and group at  $p < .001$ ; where the maximum velocity during the opening phase was consistently larger for males, larger in the vertical axis, and larger for low pitch (Figure 3). The interaction  $axis \times group$  was

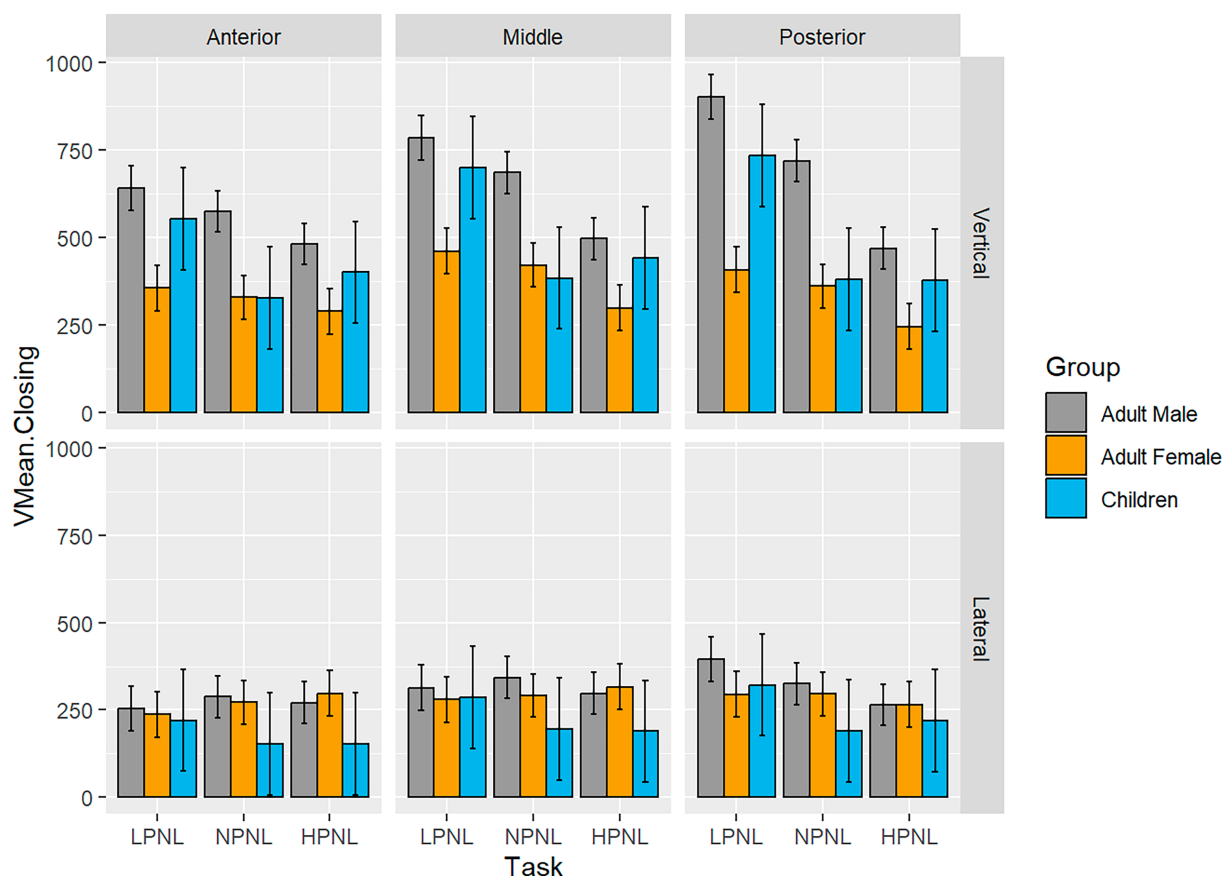


**FIGURE 6** Estimated mean and standard error of mean velocity for the closing phase (mm/s) in the lateral and vertical directions along the anterior, middle, and posterior sections of the vocal folds for low pitch normal loudness (LPNL), normal pitch normal loudness (NPNL), and high pitch normal loudness (HPNL) in males ( $n = 12$ ), females ( $n = 11$ ), and children ( $n = 2$ ).

significant ( $p = .007$ ) suggesting, that the difference in the maximum opening velocity between the groups depends on the axis; where the maximum opening velocity was significantly larger in the vertical direction for only males ( $p < .001$ ) and not significant for females ( $p = .904$ ) and children ( $p = .999$ ) when compared with lateral motion.

The difference in the maximum opening velocity across tasks depends on the axis ( $p = .023$ ) and the position ( $p = .043$ ). The maximum opening velocity is larger during the low pitch compared with normal pitch ( $p = .005$ ) and high pitch ( $p = .002$ ) in vertical axis. Similar findings were not observed for low pitch phonation when compared with normal pitch ( $p = .806$ ) and high pitch ( $p = .693$ ) in the lateral axis. Statistical significance was not obtained for maximum opening velocity between normal pitch and high pitch in the vertical ( $p = .999$ ) and lateral axis ( $p = 1$ ).

### 3.1.3 | Mean opening velocity (mm/s)

There were significant main effects of axis, task, and group; where the mean velocity during the opening phase was consistently larger for males ( $p = .01$ ), larger in the vertical axis ( $p = .003$ ), and larger for low pitch ( $p = .011$ ). No interactions were significant (Figure 4).

### 3.1.4 | Maximum closing velocity (mm/s)

Significant main effects of axis ( $p < .001$ ), task ( $p = .012$ ), group ( $p = .002$ ), and position ( $p < .001$ ) were observed for maximum closing velocity (Figure 5). Consistently, the maximum closing velocity was larger in the vertical axis, for adult males, for low pitch, and along the middle section of the vocal folds. The difference across the groups in maximum closing velocity depends on the axis ( $p = .036$ ), where the maximum closing velocity was significantly larger in the vertical direction for male ( $p < .001$ ), females ( $p = .015$ ), and children ( $p = .022$ ) when compared with lateral motion. Significant interaction of *task*  $\times$  *position* was also observed ( $p = .033$ ), where the maximum closing velocity was large along the posterior section for low pitch when compared with typical pitch ( $p = .043$ ) and high pitch ( $p < .001$ ). For low pitch, the maximum closing velocity was also higher for the middle section compared with high pitch ( $p = .025$ ).

### 3.1.5 | Mean closing velocity (mm/s)

The main effects of axis ( $p < .001$ ), group ( $p = .007$ ), and position ( $p = .003$ ) was significant for mean closing velocity, where the mean closing velocity was consistently larger for adult males, larger in the vertical axis compared with the lateral axis, and larger along the

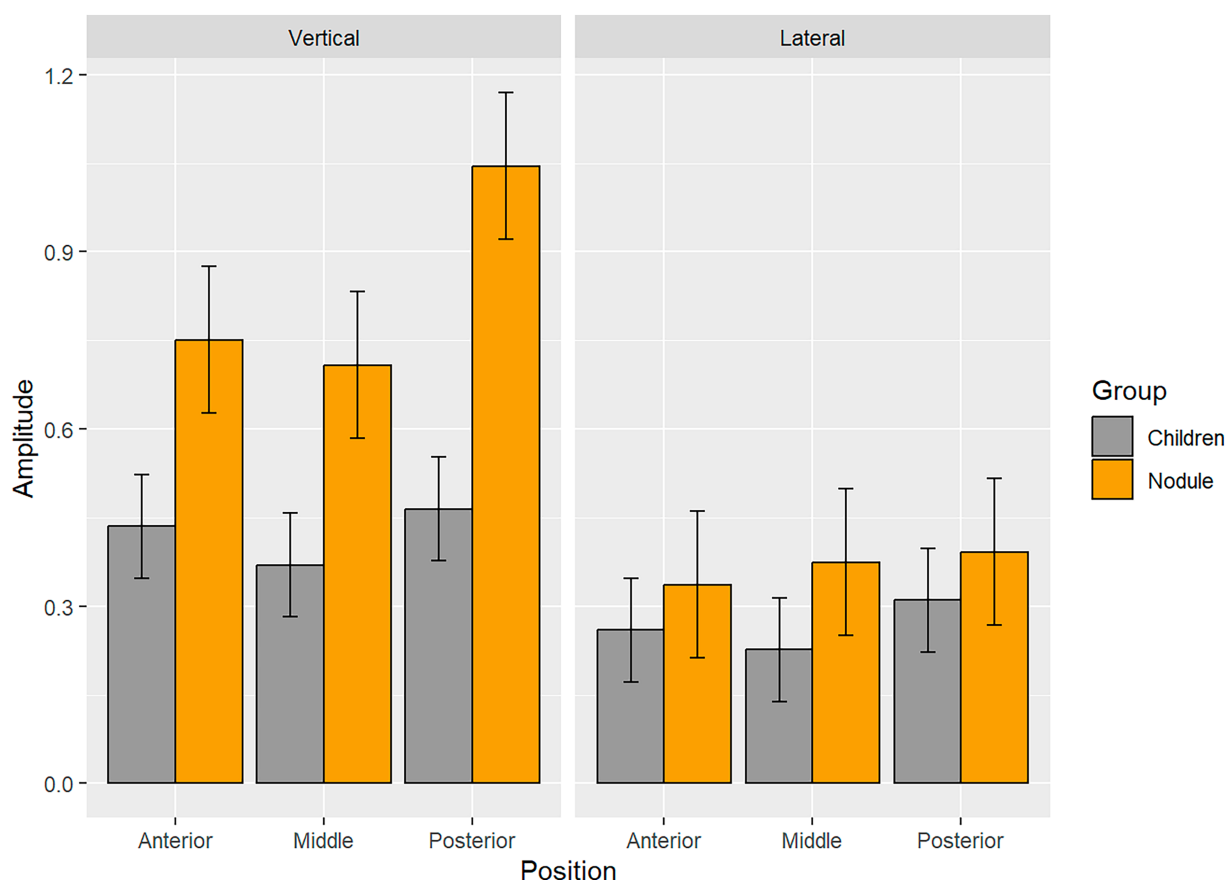


**FIGURE 7** Estimated mean and standard error of amplitude (mm) in the lateral and vertical directions along the anterior, middle, and posterior sections of the vocal folds in children ( $n = 2$ ) and a child with vocal nodules ( $n = 1$ ).

posterior section of the vocal folds when compared with middle and anterior vocal fold sections (Figure 6). The difference in the mean velocity closing between the groups depends on the axis ( $p = .046$ ), where the mean velocity closing was significantly larger in the vertical direction for male ( $p < .001$ ) and children ( $p < .001$ ) but not significant for females ( $p = .087$ ) when compared with lateral motion.

### 3.2 | Children compared with child with vocal nodules

#### 3.2.1 | Amplitude (mm)

The main effect of group ( $p = .038$ ) was significant, where amplitude was consistently larger in the child with nodules (mean = 0.60) compared with typically developing children (mean = 0.34) in both vertical and lateral motion. The amplitude was large in the vertical direction across all sections compared with the lateral motion in a child with nodules; however, this was not statistically significant (Figure 7).

#### 3.2.2 | Maximum opening velocity (mm/s)

The main effect of group ( $p = .002$ ) was significant, where the maximum opening velocity was consistently larger in the child with

nodules compared with typically developing children. The difference in the maximum opening velocity between the groups depends on axis ( $p = .017$ ) and position ( $p < .001$ ), where the maximum velocity for the opening phase was large for the visible posterior section compared with the middle section in the child with vocal nodules ( $p = .008$ ). The group difference in vertical motion was larger than the difference in the lateral motion (Figure 8).

#### 3.2.3 | Mean opening velocity (mm/s)

The main effects of group ( $p = .022$ ), axis ( $p = .019$ ), and position ( $p = .047$ ) were significant, where the mean opening velocity was consistently large in the lateral axis, larger in the child with nodules compared with typically developing children, and larger in the posterior section compared with the middle and the anterior sections of the vocal folds (Figure 9). The difference in the mean opening velocity between the groups depends on axis ( $p = .027$ ) and position ( $p < .001$ ), where the mean velocity for the opening phase was large for posterior section compared with the middle section ( $p < .001$ ) and the anterior vocal fold sections ( $p < .001$ ) in the child with vocal nodules. The interaction  $axis \times position$  was also significant ( $p < .001$ ), where the mean opening velocity is greater in the posterior portion compared with the middle portion ( $p < .001$ ) and anterior portion ( $p = .003$ ) along the vertical axis. In the lateral axis, the mean

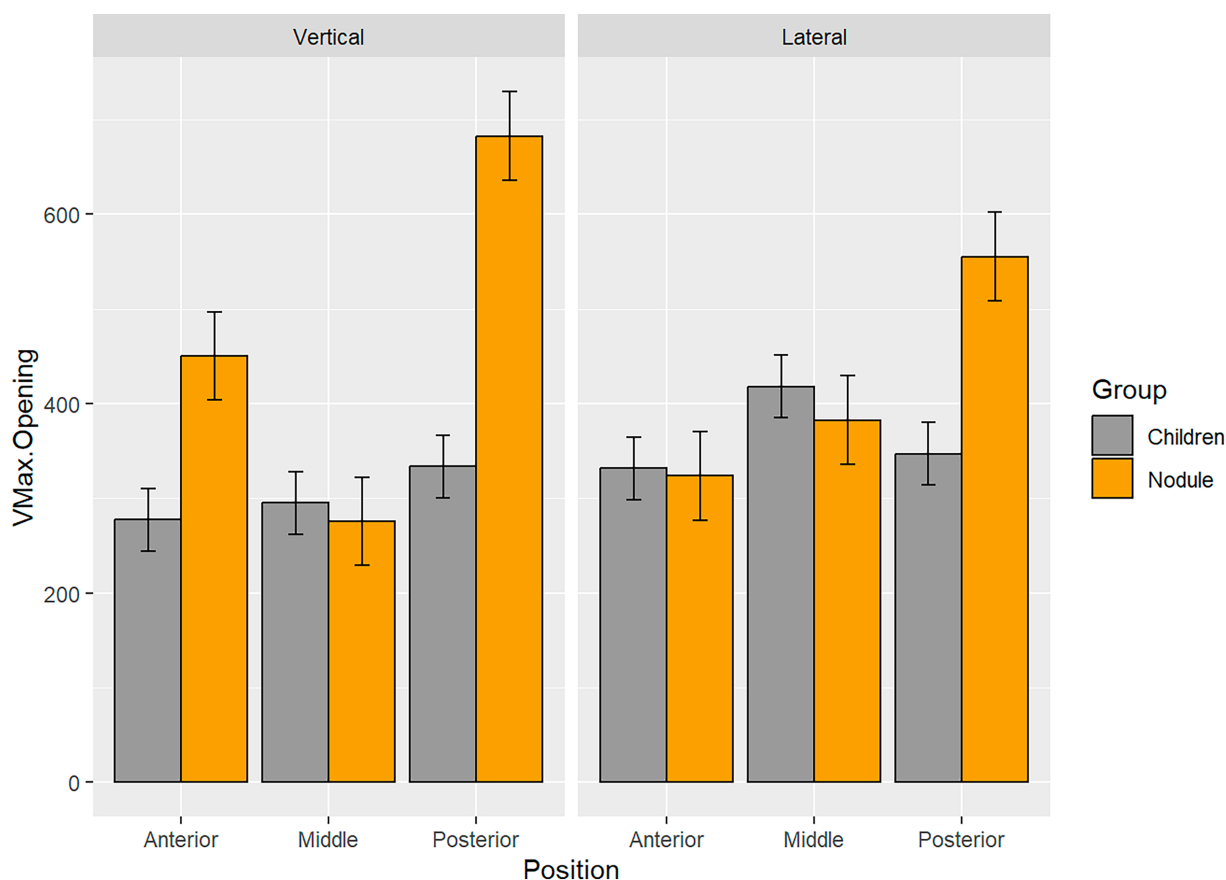


**FIGURE 8** Estimated mean and standard error of maximum velocity for the opening phase (mm) in the lateral and vertical directions along the anterior, middle, and posterior sections of the vocal folds in children ( $n = 2$ ) and a child with vocal nodules ( $n = 1$ ).

opening velocity is greater in the posterior compared with the anterior portion ( $p < .001$ ) and greater in the middle portion compared with the anterior portion ( $p = .008$ ).

### 3.2.4 | Maximum closing velocity (mm/s)

The main effects of axis ( $p = .284$ ), group ( $p = .426$ ), and position ( $p = .871$ ) were not significant for maximum closing velocity (Figure 10).

### 3.2.5 | Mean closing velocity (mm/s)

The main effects of axis ( $p = .159$ ), group ( $p = .236$ ), and position ( $p = .879$ ) were not significant for mean closing velocity (Figure 11).

## 4 | DISCUSSION

The study demonstrates the first in vivo measurements of the superior surface vocal fold dynamics in children (Figure 12) with the multi-array laser coupled with high-speed system in children.

### 4.1 | 3D vibratory dynamics in typically developing children

Overall, the vertical motion along the superior surface of the vocal folds was consistently larger in the closing phase compared with the lateral motion in children, adult males, and adult females. A reviewer suggests that there is no statistical significance; however, we disagree as the maxing closing velocity and the mean closing velocity are significantly larger in the vertical direction compared with the lateral direction, suggesting that the superior surface undergoes more significant vertical motion during the final phase of the glottal cycle. The findings from the current study of large vertical motion compared with the lateral motion are similar to the findings of in vivo<sup>27,31,32,46</sup> in adults and ex-vivo<sup>26,47</sup> use of laser projection. Nevertheless, the present study is the initial one to illustrate this phenomenon in vocally healthy children. The vertical motion was especially more pronounced along the visible posterior section of the vocal folds during low pitch phonation compared with females; provide the impression that the vertical motion in typically developing children resembles that of adult males more than adult females. A similar pattern of children's vibratory motion more closely resembling that of adult males was also observed in kinematic studies that utilized only high-speed videoendoscopy to evaluate the lateral motion.<sup>21,23</sup>

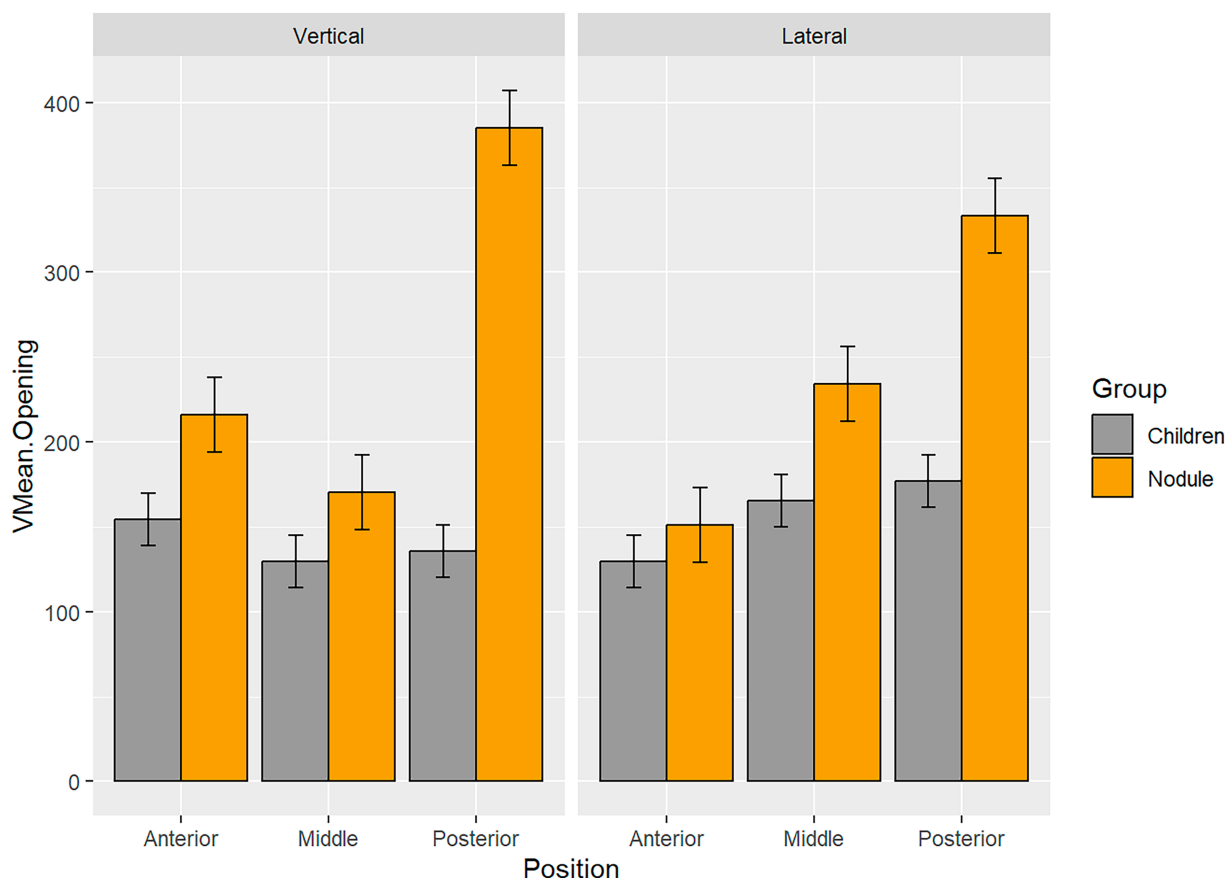


**FIGURE 9** Estimated mean and standard error of mean velocity for the opening phase (mm) in the lateral and vertical directions along the anterior, middle, and posterior sections of the vocal folds in children ( $n = 2$ ) and a child with vocal nodules ( $n = 1$ ).



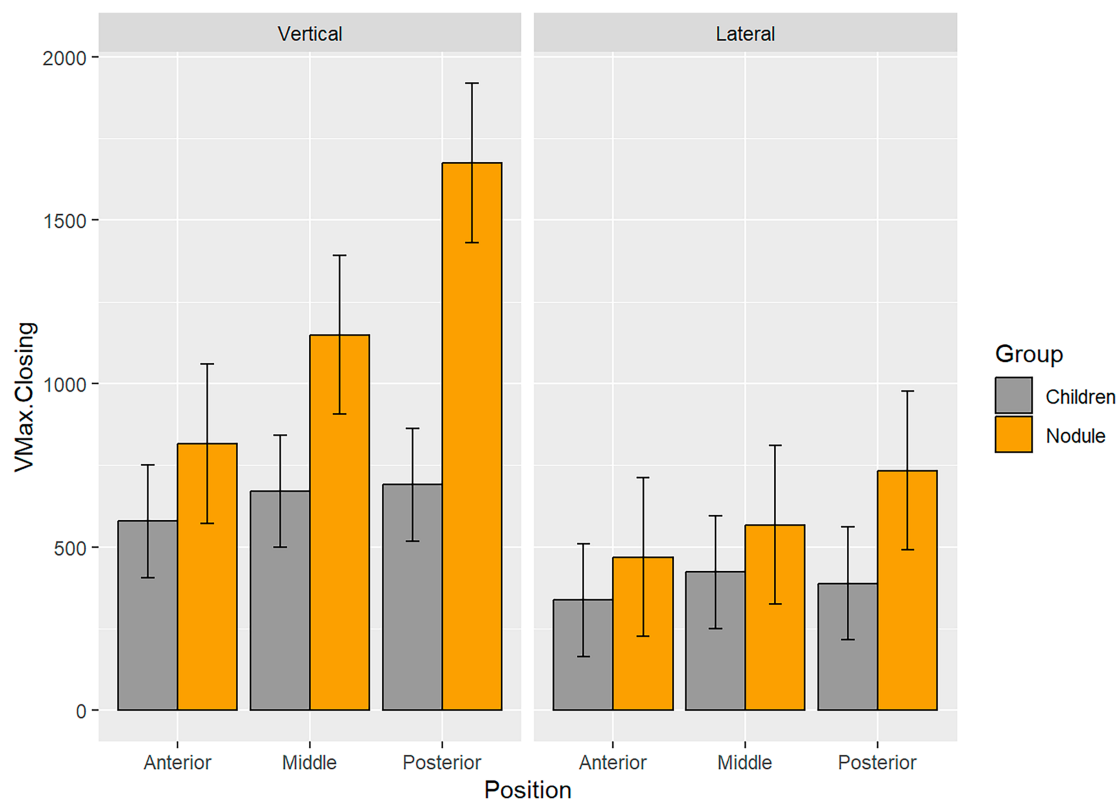


**FIGURE 10** Estimated mean and standard error of maximum velocity for the closing phase (mm) in the lateral and vertical directions along the anterior, middle, and posterior sections of the vocal folds in children ( $n = 2$ ) and a child with vocal nodules ( $n = 1$ ).

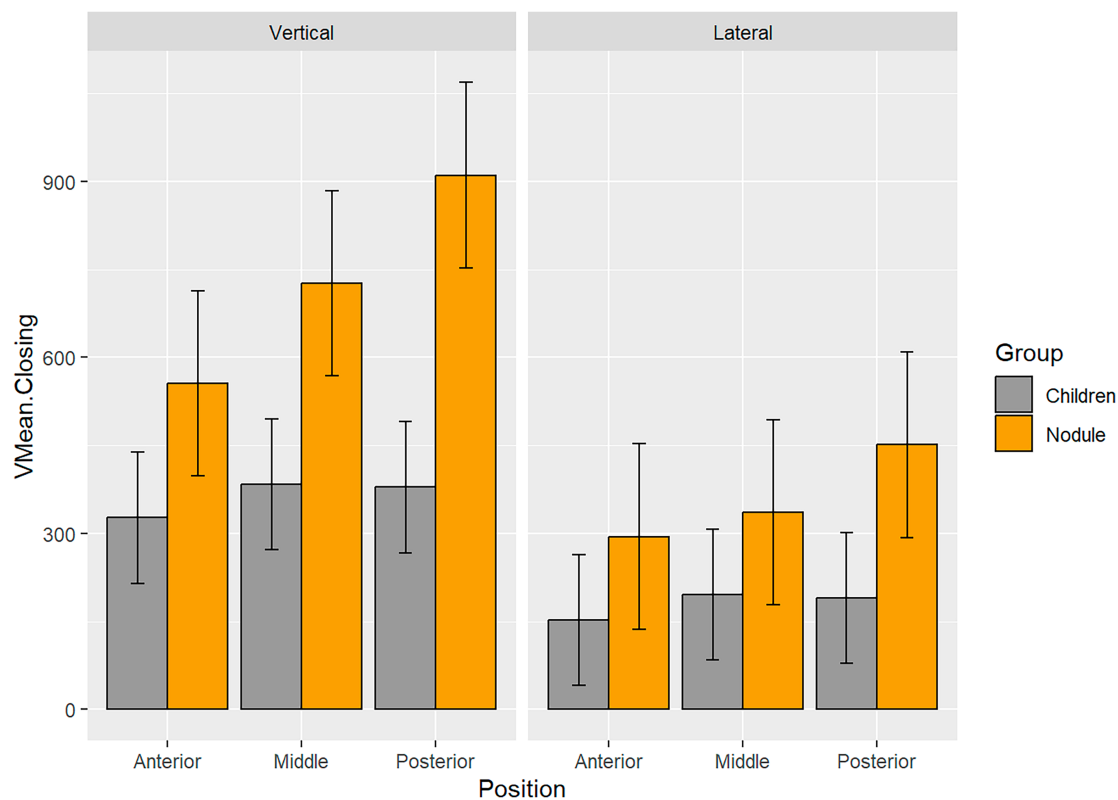


**FIGURE 11** Estimated mean and standard error of mean velocity for the closing phase (mm) in the lateral and vertical directions along the anterior, middle, and posterior sections of the vocal folds in children ( $n = 2$ ) and a child with vocal nodules ( $n = 1$ ).

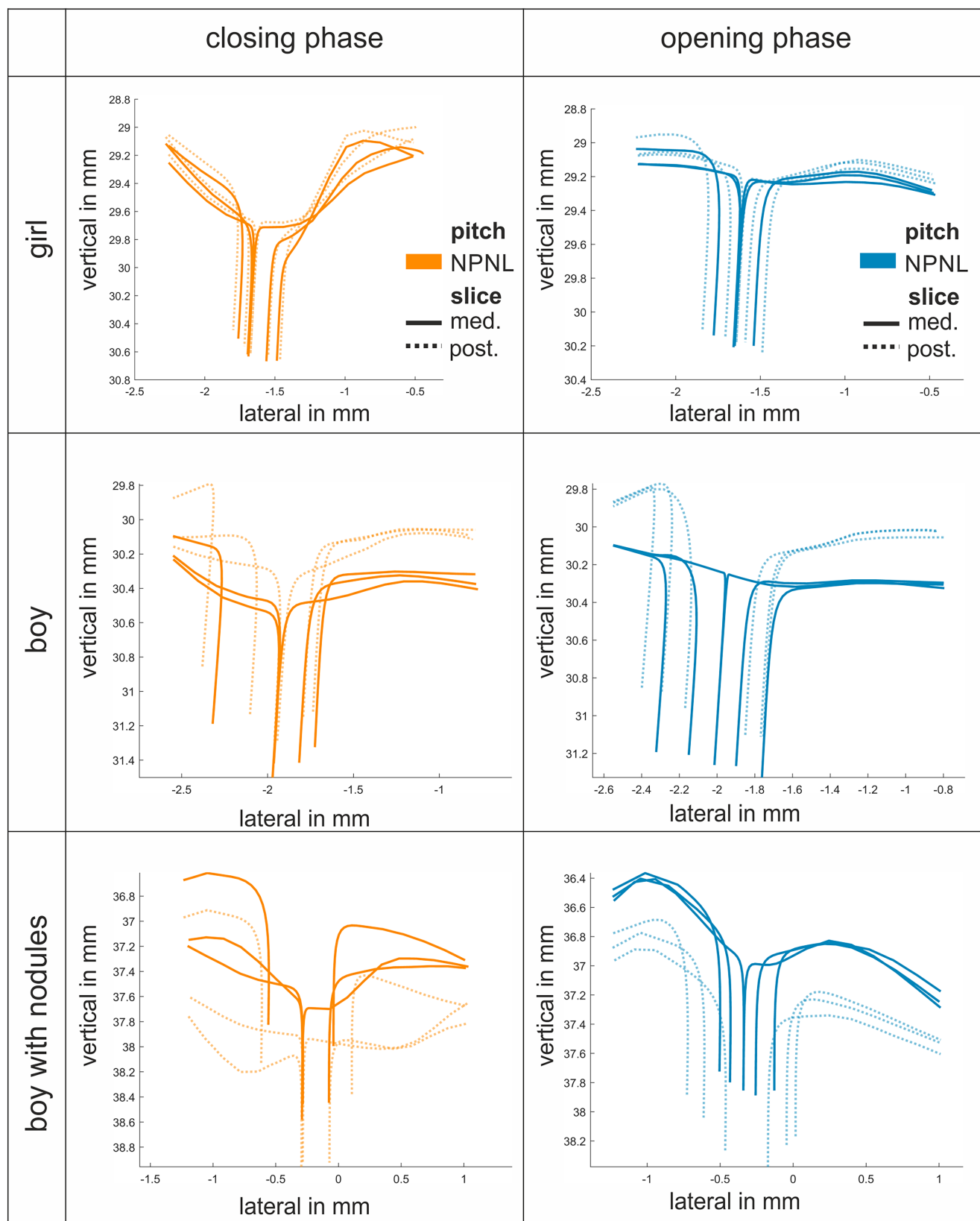


**FIGURE 12** Typical results from vocally normal children, and a child with vocal nodules showing the lateral and vertical motion for typical pitch along the middle, and posterior sections of the vocal folds in opening and closing phase.

The study provides preliminary evidence of the importance of quantifying closing phase dynamics compared with the opening phase dynamics when evaluating developmental differences between children without any voice problems.

## 4.2 | 3D vibratory dynamics in a child with vocal nodules

The study findings from this one child with nodule when compared with 2 typically developing children reveal the 3D amplitude, maximum opening velocity, and mean opening velocity were significantly larger in the child with nodules compared with vocally normal children. These findings are consistent with biomechanical modeling studies which showed increased amplitude<sup>48</sup> but contrary to those that showed high vocal fold closing velocity laterally.<sup>18,42</sup> To the best of our knowledge, there are no other studies that have looked at quantifying vibratory motion in children. Although the absence of statistical significance in the closing phase in a child with vocal nodules may be attributed to the single subject in the study, the strength of this discovery becomes evident when compared with typically developing children. The lack of statistical significance in the closing phase dynamics could also be attributed to the large standard errors, resulting in overlapping confidence intervals for the closing phase dynamics. The study also consistently reports larger amplitude, maximum/mean opening velocity along the visible posterior section in children with vocal nodules, suggesting the importance of investigating not only the mid-membranous dynamics but also the posterior vocal fold section dynamics in children with large number of participants. As the reviewer suggested, this discussion offers limited explanations for the results in children, because, to the best of our knowledge, no previous studies have quantified 3D motion in children.

## 4.3 | Limitations and future needs

Although this is a prospective study, the study is limited by small number of children participants. Future studies should aim to replicate the findings with larger sample sizes to enhance the generalizability of the results. The child with nodule only produced typical phonation. Future studies need to evaluate the changes in 3D vertical motion across variations in pitch and loudness in children with vocal nodules in large sample sizes.

## 5 | CONCLUSIONS

The custom laser device was successfully used to quantify the 3D motion of the vocal folds in vivo in children. This establishes the feasibility of capturing 3D motion in a clinical setting and provides proof of concept for the application of the proposed 3D laser in the pediatric population. The preliminary findings underscore the need to evaluate

the 3D vertical motion along the superior surface in the closing phasing phase to distinguish vibratory motion between children and adults and emphasize the significance of studying posterior motion in children with vocal nodules during the opening phase. Despite the small sample size, the study findings offer a foundation for further research into the complex vertical and lateral vocal fold dynamics observed in vocally normal children and a child with vocal nodules.

## ACKNOWLEDGEMENTS

We thank the Indiana University Biostatistical Consulting for their assistance with statistical analyses and Tzu Pei Tsai, Caroline Riefe for their assistance with data segmentation. Contributions by R Patel were supported by NIH NIDCD R01DC017923 and by M Semmler & M Döllinger were supported by Deutsche Forschungsgemeinschaft (DFG) under grant no. DO1247/16-1.

## FUNDING INFORMATION

NIH NIDCD (R01DC017923) and DFG (DO 1247/16-1).

## ORCID

Rita R. Patel  <https://orcid.org/0000-0002-5354-5210>

Marion Semmler  <https://orcid.org/0000-0001-6753-8102>

## REFERENCES

1. Stachler RJ, Francis DO, Schwartz SR, et al. Clinical practice guideline: hoarseness (Dysphonia) (update). *Otolaryngol Head Neck Surg*. 2018; 158(1\_suppl):S1-S42. doi:[10.1177/0194599817751030](https://doi.org/10.1177/0194599817751030)
2. Patel RR, Awan SN, Barkmeier-Kraemer J, et al. Recommended protocols for instrumental assessment of voice: american speech-language-hearing association expert panel to develop a protocol for instrumental assessment of vocal function. *Am J Speech Lang Pathol*. 2018;25:1-19. doi:[10.1044/2018\\_AJSLP-17-0009](https://doi.org/10.1044/2018_AJSLP-17-0009)
3. Patel RR, Dailey S, Bless D. Comparison of high-speed digital imaging with stroboscopy for laryngeal imaging of glottal disorders. *Ann Otol Rhinol Laryngol*. 2008;117(6):413-424.
4. Olthoff A, Woywod C, Kruse E. Stroboscopy versus high-speed laryngography: A comparative study. *Laryngoscope*. 2007;117(6):1123-1126. doi:[10.1097/Mlg.0b013e318041f70c](https://doi.org/10.1097/Mlg.0b013e318041f70c)
5. Chen W, Woo P, Murry T. Spectral analysis of digital kymography in normal adult vocal fold vibration. *J Voice*. 2014;28(3):356-361. doi:[10.1016/j.jvoice.2013.10.015](https://doi.org/10.1016/j.jvoice.2013.10.015)
6. Mehta DD, Zaeartu M, Quatieri TF, Deliyski DD, Hillman RE. Investigating acoustic correlates of human vocal fold vibratory phase asymmetry through modeling and laryngeal high-speed videoendoscopy. Research Support, N.I.H., Extramural Research Support, Non-U.S. Gov't Research Support, U.S. Gov't, Non-P.H.S. *J Acoust Soc Am*. 2011;130(6):3999-4009. doi:[10.1121/1.3658441](https://doi.org/10.1121/1.3658441)
7. Bonilha HS, Deliyski DD. Period and glottal width irregularities in vocally normal speakers. *J Voice*. 2008;22(6):699-708. doi:[10.1016/j.jvoice.2007.03.002](https://doi.org/10.1016/j.jvoice.2007.03.002)
8. Bonilha HS, Deliyski DD, Gerlach TT. Phase asymmetries in normophonic speakers: visual judgments and objective findings. *Am J Speech Lang Pathol*. 2008;17(4):367-376. doi:[10.1044/1058-0360\(2008\)07-0059](https://doi.org/10.1044/1058-0360(2008)07-0059)
9. Patel RR, Liu L, Galatsanos NP, Bless D. Differential vibratory characteristics of adductor spasmodic dysphonia and muscle tension dysphonia on high-speed digital imaging. *Ann Otol Rhinol Laryngol*. 2011; 120(1):21-32.

10. Patel RR, Walker R, Döllinger M. Oscillatory onset and offset in young vocally healthy adults across various measurement methods. *J Voice*. 2017;31:512. doi:[10.1016/j.jvoice.2016.12.002](https://doi.org/10.1016/j.jvoice.2016.12.002)
11. Patel RR, Sandage MJ, Golzarri-Arroyo L. High-speed videoendoscopic and acoustic characteristics of inspiratory phonation. *J Speech Lang Hear Res*. 2023;66(4):1192-1207. doi:[10.1044/2022\\_JSLHR-22-00502](https://doi.org/10.1044/2022_JSLHR-22-00502)
12. Mendelsohn AH, Remacle M, Courey MS, Gerhard F, Postma GN. The diagnostic role of high-speed vocal fold vibratory imaging. *J Voice*. 2013;20:2130. doi:[10.1016/j.jvoice.2013.04.011](https://doi.org/10.1016/j.jvoice.2013.04.011)
13. Mehta DD, Deliyiski DD, Zeitels SM, Quatieri TF, Hillman RE. Voice production mechanisms following phonosurgical treatment of early glottic cancer. *Ann Otol Rhinol Laryngol*. 2010;119(1):1-9.
14. Powell ME, Deliyiski DD, Hillman RE, Zeitels SM, Burns JA, Mehta DD. Comparison of videostroboscopy to stroboscopy derived from high-speed videoendoscopy for evaluating patients with vocal fold mass lesions. *Am J Speech Lang Pathol*. 2016;25(4):576-589. doi:[10.1044/2016\\_AJSLP-15-0050](https://doi.org/10.1044/2016_AJSLP-15-0050)
15. Patel RR, Pickering J, Stemple J, Donohue KD. A case report in changes in phonatory physiology following voice therapy: application of high-speed imaging. *J Voice*. 2012;20:205. doi:[10.1016/j.jvoice.2012.01.001](https://doi.org/10.1016/j.jvoice.2012.01.001)
16. Zacharias SR, Myer CM, Meinzen-Derr J, Kelchner L, Deliyiski DD, de Alarcon A. Comparison of videostroboscopy and high-speed videoendoscopy in evaluation of supraglottic phonation. *Ann Otol Rhinol Laryngol*. 2016;125(10):829-837. doi:[10.1177/0003489416656205](https://doi.org/10.1177/0003489416656205)
17. Patel RR. Vibratory onset and offset times in children: A laryngeal imaging study. *Int J Pediatr Otorhinolaryngol*. 2016;87:11-17.
18. Patel RR, Unnikrishnan H, Donohue KD. Effects of vocal fold nodules on glottal cycle measurements derived from high-speed videoendoscopy in children. *PLoS One*. 2016;11(4):e0154586. doi:[10.1371/journal.pone.0154586](https://doi.org/10.1371/journal.pone.0154586)
19. Döllinger M, Dubrovskiy D, Patel RR. Spatiotemporal analysis of vocal fold vibrations between children and adults. *Laryngoscope*. 2012; 122(11):2511-2518. doi:[10.1002/lary.23568](https://doi.org/10.1002/lary.23568)
20. Patel RR, Dixon A, Richmond A, Donohue KD. Pediatric high speed digital imaging of vocal fold vibration: A normative pilot study of glottal closure and phase closure characteristics. *Int J Pediatr Otorhinolaryngol*. 2012;76:954-959.
21. Patel RR, Dubrovskiy D, Döllinger M. Measurement of glottal cycle characteristics between children and adults: physiological variations. *J Voice*. 2014;28(4):476-486. doi:[10.1016/j.jvoice.2013.12.010](https://doi.org/10.1016/j.jvoice.2013.12.010)
22. Unnikrishnan H, Donohue KD, Patel RR. Analysis of high-speed phonoscopy pediatric images. *Proc Int Soc Optics Photonics SPIEberg*. 2012;8207:11-13.
23. Patel RR, Donohue KD, Unnikrishnan H, Kryscio RJ. Kinematic measurements of the vocal-fold displacement waveform in typical children and adult populations: quantification of high-speed endoscopic videos. *J Speech Lang Hear Res*. 2015;58(2):227-240. doi:[10.1044/2015\\_JSLHR-S-13-0056](https://doi.org/10.1044/2015_JSLHR-S-13-0056)
24. Semmler M, Kniesburges S, Birk V, Ziethe A, Patel RR, Döllinger M. 3D reconstruction of human laryngeal dynamics based on endoscopic high-speed recordings. *IEEE Trans Med Imaging*. 2016;35(7):1615-1624. doi:[10.1109/TMI.2016.2521419](https://doi.org/10.1109/TMI.2016.2521419)
25. Henningson J-O, Stamminger M, Doellinger M, Semmler M. Real-time 3d reconstruction of human vocal folds via high-speed laser-endoscopy. *Medical Image Computing and Computer Assisted Intervention-MICCAI 2022: 25th International Conference, Singapore, September 18-22, 2022, Proceedings*. Springer; 2022:3-12.
26. Luegmair G, Mehta DD, Kobler JB, Döllinger M. Three-dimensional optical reconstruction of vocal fold kinematics using high-speed video with a laser projection system. *IEEE Trans Med Imaging*. 2015;34(12): 2572-2582. doi:[10.1109/TMI.2015.2445921](https://doi.org/10.1109/TMI.2015.2445921)
27. Semmler M, Döllinger M, Patel RR, Ziethe A, Schutzenberger A. Clinical relevance of endoscopic three-dimensional imaging for quantitative assessment of phonation. *Laryngoscope*. 2018;128:2367-2374. doi:[10.1002/lary.27165](https://doi.org/10.1002/lary.27165)
28. Semmler M, Kniesburges S, Parchent J, et al. Endoscopic laser-based 3D imaging for functional voice diagnostics. *Appl Sci-Basel*. 2017;7(6): Art n 600.
29. Schuberth S, Hoppe U, Döllinger M, Lohscheller J, Eysholdt U. High-precision measurement of the vocal fold length and vibratory amplitudes. *Laryngoscope*. 2002;112(6):1043-1049. doi:[10.1097/00005537-200206000-00020](https://doi.org/10.1097/00005537-200206000-00020)
30. Popolo PS, Titze IR. Qualification of a quantitative laryngeal imaging system using videostroboscopy and videokymography. *Ann Otol Rhinol Laryngol*. 2008;117(6):404-412.
31. Larsson H, Hertegard S. Calibration of high-speed imaging by laser triangulation. *Logoped Phoniatr Vocol*. 2004;29(4):154-161.
32. Patel RR, Döllinger M, Jakubass B, Pinhack MD, Katz U, Semmler M. Analyzing vocal fold frequency dynamics using high-speed 3D laser video endoscopy. *Laryngoscope*. 2024; 134:3267-3276.
33. Boseley ME, Hartnick CJ. Development of the human true vocal fold: depth of cell layers and quantifying cell types within the lamina propria. *Ann Otol Rhinol Laryngol*. 2006;115(10):784-788.
34. Hartnick CJ, Rehbar R, Prasad V. Development and maturation of the pediatric human vocal fold lamina propria. *Laryngoscope*. 2005;115(1): 4-15.
35. Sato K, Hirano M, Nakashima T. Fine structure of the human newborn and infant vocal fold mucosae. *Ann Otol Rhinol Laryngol*. 2001;110(5 Pt 1):417-424.
36. Hirano M, Kurita S, Nakashima T. Growth, development, and aging of human vocal fold. In: Bless DM, Abbs JH, eds. *Vocal Physiology contemporary research and clinical issues*. College-Hill Press; 1983:22-43.
37. Kahane JC. A morphological study of the human prepubertal and pubertal larynx. *Am J Anat*. 1978;151(1):11-19. doi:[10.1002/aja.1001510103](https://doi.org/10.1002/aja.1001510103)
38. Kahane JC. Growth of the human prepubertal and pubertal larynx. *J Speech Hear Res*. 1982;25(3):446-455.
39. Eckel HE, Koebke J, Sittel C, Sprinzl GM, Pototschnig C, Stennert E. Morphology of the human larynx during the first five years of life studied on whole organ serial sections. *Ann Otol Rhinol Laryngol*. 1999;108(3):232-238.
40. Correction: BTS clinical statement on pulmonary sarcoidosis. *Thorax*. 2021;76(7):e4. doi:[10.1136/thoraxjnl-2019-214348corr1](https://doi.org/10.1136/thoraxjnl-2019-214348corr1)
41. Patel, RR, Donohue, KD, Johnson WC, Archer SM. Laser projection imaging for measurement of pediatric voice. Research Support, N.I.H., Extramural Research Support, Non-U.S. Gov't. *Laryngoscope*. 2011; 121(11):2411-2417. doi:[10.1002/lary.22325](https://doi.org/10.1002/lary.22325)
42. Patel RR, Donohue KD, Lau D, Unnikrishnan H. In vivo measurement of pediatric vocal fold motion using structured light laser projection. *J Voice*. 2013;27(4):463-472.
43. Patel RR, Unnikrishnan H, Donohue D. Measurement of lesion size and characterization of vibratory dynamics in a male child with vocal fold nodules before and after voice therapy. *Normal and Abnormal Vocal Fold Kinematics, High-Speed Digital Phonoscopy, Optical Coherence Tomography & Narrow Band Imaging*. CreateSpace Independent Publishing Platform; 2016:189-197.
44. Lohscheller J, Toy H, Rosanowski F, Eysholdt U, Döllinger M. Clinically evaluated procedure for the reconstruction of vocal fold vibrations from endoscopic digital high-speed videos. Research Support, Non-U.S. Gov't. *Med Image Anal*. 2007;11(4):400-413. doi:[10.1016/j.media.2007.04.005](https://doi.org/10.1016/j.media.2007.04.005)
45. Kist AM, Gomez P, Dubrovskiy D, et al. A deep learning enhanced novel software tool for laryngeal dynamics analysis. *J Speech Lang Hear Res*. 2021;64(6):1889-1903. doi:[10.1044/2021\\_JSLHR-20-00498](https://doi.org/10.1044/2021_JSLHR-20-00498)
46. Wurzbacher T, Voigt I, Schwarz R, et al. Calibration of laryngeal endoscopic high-speed image sequences by an automated detection of parallel laser line projections. *Med Image Anal*. 2008;12(3):300-317.

47. Luegmair G, Kniesburges S, Zimmermann M, Sutor A, Eysholdt U, Döllinger M. Optical reconstruction of high-speed surface dynamics in an uncontrollable environment. Research Support, Non-U.S. Gov't. *IEEE Trans Med Imaging*. 2010;29(12):1979-1991. doi:[10.1109/TMI.2010.2055578](https://doi.org/10.1109/TMI.2010.2055578)
48. Dejonckere PH, Kob M. Pathogenesis of vocal fold nodules: new insights from a modelling approach. *Folia Phoniatr Logop*. 2009;61(3):171-179. doi:[10.1159/000219952](https://doi.org/10.1159/000219952)

**How to cite this article:** Patel RR, Döllinger M, Semmler M. 3D reconstruction of vocal fold dynamics with laser high-speed videoendoscopy in children. *Laryngoscope Investigative Otolaryngology*. 2024;9(5):e70024. doi:[10.1002/liv.2.70024](https://doi.org/10.1002/liv.2.70024)